Proceedings of the IMECE'01
International Mechanical Engineering Congress and Exposition (IMECE)
New York, New York USA November 11-16, 2001

DESIGN OF A MICRO DIRECT METHANOL FUEL CELL (μDMFC)

M. M. Mench, Z. H. Wang, K. Bhatia, and C. Y. Wang
Electrochemical Engine Center
Department of Mechanical and Nuclear Engineering
Pennsylvania State University
University Park, PA 16802, USA
Tel: +1-814-865-0060
Fax: +1-814-863-4848
Email: mmm124@psu.edu

ABSTRACT

Recently, there has been increased interest in the development of a small-sized direct methanol fuel cell (DMFC) for low-power applications. In this paper, the design of a self-activated DMFC stack is presented. Gravitational and capillary forces feed the anode side liquid methanol solution. On the cathode side, air is supplied by thermal and solutal buoyancy forces. Based upon experimental results for a larger test cell, and calculated flow velocities for the small-cell design, the fuel and oxidizer supply rates should be adequate for acceptable performance. The entire DMFC is therefore a pump-less operation and self-activated by electrochemical reactions. At 1 cm^3 total volume, the DMFC is expected to provide a power density around 1 W/cm^3, with a range of output of 10V, 0.1A to 1 V, 1A depending on the arrangement of individual cell connections.

NOMENCLATURE

A Area term, cm^2
c molar concentration, mol/cm^3
cp specific heat, J/mole K
D channel hydraulic diameter, cm
F Faraday constant, 96,487 As/eq
g gravitational constant, 9.81 m/s^2
H Channel height, cm
I current density, A/cm^2
L flow channel length, cm
M molecular weight
P pressure, Pa
R gas constant, 8.314 J/mol·K
T temperature, K
U velocity, cm/s
V potential, V
W channel width, cm
y_{sat} distance along cathode flow path until flow is fully saturated, cm

Greek letters

α average void fraction, or effective water transport coefficient per proton through electrolyte membrane, unitless
β volumetric thermal expansion coefficient, K^{-1}
μ viscosity, g/cm·s
ν kinematic viscosity, cm^2/s
η energy efficiency of DMFC
ρ density, g/cm^3
$\bar{\rho}$ average density, g/cm^3
ζ stoichiometric flow ratio

Subscripts

a anode
atm atmospheric
c cathode
cell fuel cell
ch flow channel
f fuel
g gas-phase
in inlet
k species
l liquid-phase
ref reference value
rxn electrochemical reaction
sto stoichiometric conditions
sat saturation condition
∞ ambient

Superscripts

air air
H_2O water
MeOH methanol

INTRODUCTION

In recent years, tremendous interest in the potential use of fuel cell systems for a variety of power generation applications has arisen. The benefits of fuel cell systems include increased power and energy densities, higher efficiency, silent operation, environmentally benign emissions, low temperature operation, and modularity of design. Unlike a hydrogen polymer electrolyte fuel cell (H_2 PEMFC), the direct methanol fuel cell (DMFC) does not require ancillary components such as a separate humidifier, fuel processor, or cooling system. In addition, use of dense liquid fuel at atmospheric pressure eliminates the need for bulky fuel storage tanks. Even at 50% efficiency, one ml of methanol can deliver about 2.5 Watt-hours of electricity. Because of these qualities, DMFCs are ideally suited for electronic applications typically powered by electrochemical battery systems.

There have been significant ongoing activities in the United States and around the world to develop large-scale DMFC technology. Preliminary studies have been performed on large-scale (> 1 cm^2 active area) DMFC systems by Surampudi and coworkers (Surampudi et al. 1994), Halpert and coworkers (Halpert et al. 1997) at the Jet Propulsion Laboratory, Ren and coworkers (Ren et al. 2000) at Los Alamos National Laboratory, and Wang and coworkers (Wang et al. 2001) at the Penn State University Electrochemical Engine Center. While these studies on macro-systems show great promise of DMFC technology, its application to portable and MEMS power sources is not straightforward, in view of the fundamental differences between macro- and micro-systems.

There has also been significant effort made to develop micro fuel cells for MEMS applications; notable efforts include those by Savinell and co-workers at Case Western Reserve University to develop a micro hydrogen PEM fuel cell. This design suffers a low energy density due to the significant limitation posed by hydrogen storage. The micro direct methanol fuel cell concept is currently being aggressively pursued by several organizations including Motorola (Bostaph et al., 2001), JPL (Narayanan et al., 2001) and University of Minnesota (Kelly et al., 2000). Motorola has already demonstrated a DMFC that relies on external pumping with a net power density 15 mW/cm^2. JPL has demonstrated a DMFC with an even lower power density of 8 mW/cm^2, in a design where methanol feed is accomplished by diffusion. This is in an attempt to eliminate the parasitic power loss. It is clear from these two studies that the liquid fuel feed is an important process affecting the power density.

As a result of the relatively poor performance demonstrated so far, there is a great need for advanced design of small-scale DMFC systems for use as power source in electronic systems with low parasitic losses for increased power density. This work is motivated by the need for an improved small-scale DMFC design for increased power density.

The proposed DMFC design is pump-less and self-activated by electrochemical reactions. The fuel in the anode channel is driven by the buoyancy and capillary forces resulting from the gradient in the bubble void fraction along the flow channel. The resulting fuel flow requires no parasitic power consumption. Oxidant flow is provided by thermal and solutal buoyancy forces, as ambient air becomes warmer and more moist when traveling through the flow channel. In addition, since the liquid methanol also acts as a coolant for the stack, the DMFC can be effectively cooled by the liquid fuel itself. Hence, both air and fuel supply as well as stack cooling are achieved without any parasitic power losses.

DMFC STACK DESIGN

A design drawing of the DMFC fuel cell stack, including fuel reserve tank and feed system, is shown in Figure 1. A top down and a bottom up perspective are shown to enhance clarity. The entire system is shown, in this case consisting of a 20-cell direct methanol fuel cell (DMFC) stack with the total volume of around 1 cm^3 (~ 1 cm high by 1 cm wide by 1 cm deep), including methanol solution reservoir, fuel supply manifold system, and manifold interface with the fuel cell. If additional fuel storage is desired, the height of the fuel tank can be increased accordingly. Depending on the application, the stack size can be increased or decreased accordingly. It is envisioned that the fuel reservoir will circulate within the cell until depletion, to be replaced with another solution cartridge that would interface with the top of the stack design shown in Fig. 1.

Figure 2 is a schematic of the fuel supply tank and feed system shown in Fig. 1 as part of the fuel cell stack. The top row of inlet holes that interface with the anode exit ports of the DMFC stack can be seen. Figures 3 and 4 are schematics of the anode and cathode flow plates, respectively. Flow plate channel and current collector rib dimensions are chosen based on existing design, and to provide both adequate contact area for rib surfaces as well as adequate flow area for membrane contact and low pressure losses. Table 1 lists relevant dimensions of the DMFC stack. It should be noted that the power density of this design relies on the ability to manufacture bipolar plates and membrane electrode assemblies with reduced thicknesses, compared to that used in larger sized DMFCs. While current MEMS technology should be able to accomplish this task, production of the

proposed stack with Nafion 117 and conventional machining techniques would increase the width of the stack twofold for the same power output.

The liquid methanol solution is primarily fed by gravity, taking advantage of bubble formation from the anode electrochemical reaction upon closed circuit. For small length scales, the gravity-driven circulation of methanol can be further enhanced by capillary forces induced by gas-liquid two-phase flow through small anode channels with geometry promoting capillary action.

The cathode air supply is designed to rely on thermal and solutal buoyancy forces. The ambient air becomes warmer and more moist when it travels through the cathode channel, promoting a density-driven flow of ambient air through the cathode channels. Therefore, the entire DMFC is a pump-less operation and self-activated by electrochemical reactions. When the cell is at open circuit, no carbon dioxide bubbles are produced, so that the anode will be dormant. On the cathode side, until the circuit is closed there will be no water vapor production or temperature gradient to induce buoyancy forces, rendering the cathode dormant as well.

On the anode side, the methanol solution flows from the supply reservoir to the lower inlet manifold on the center strip of the bottom of the fuel cell, as shown in Fig. 1. The only interface between the anode solution lines and the fuel cell is along the center strips at the top and bottom of the fuel cell. This way, anode and cathode effluent are effectively separated. The methanol solution enters the center section and is distributed to the parallel flow channels shown in Fig. 3. Within the fuel cell along the anode flow path, carbon dioxide bubbles are formed by the anodic methanol oxidation reaction, shown as:

$$CH_3OH + H_2O \rightarrow 6e^- + 6H^+ + CO_2 \qquad (1)$$

The production of the CO_2 bubbles force the flow upward to the exit of the anode plate. This two-phase flow lowers the mean density in the anode channels compared to the single-phase supply lines, providing a natural driving force for fluid motion in the anode side of the fuel cell. At the top of the anode flow plate, the flow is then redistributed back into a single channel and exits at the interface with the anode supply tank shown in Figs. 1 and 2 along the top center of the fuel cell. The carbon dioxide gas exits from anode side as well, and leaves the assembly through small openings in the top of the supply tank.

On the cathode side, air is forced, primarily by natural convection, from the ambient into the parallel cathode flow channels of the fuel cell, which are shown at the bottom of Fig. 4. The flow then proceeds upward and out of the fuel cell back to the ambient through the space between the top of the fuel cell and the fuel solution storage tank, as shown in Fig. 1. At the top of the flow plate shown in Fig. 4, the two middle gas channels are diverted away from the midplane of the fuel cell to avoid interference with the anode/fuel tank interface.

A design temperature of 80°C is chosen, based upon the desired output of 1 W. The operational design point is set at 100 mA/cm^2 @ 0.5V, which is achievable according to the latest test data from a large cell of 50 cm^2 at Penn State Electrochemical Engine Center (ECEC). Figure 5 is a DMFC polarization curve at 80°C taken at the ECEC. Although the operating cathode pressure is higher for the case shown, it is believed that the design set point output can be obtained, especially considering that the performance of DMFCs generally improves as the size is reduced, a result of more uniform temperature and species profiles.

The DMFC of 1 cm^3 (~ 1 cm high by 1 cm wide by 1 cm deep) is expected to provide a power source of 1 W with either 10V, 0.1A if all 20 cells are connected in series, or 1V, 1A if 10 cells are connected in parallel and every pair of cells is connected in series. Ultimately, this can be configured to suit specific power requirements.

Gravity-Driven Feed of Anode Methanol Solution Fuel

The mechanism of gravity-feed of liquid methanol is schematically shown in Figure 6, which shows a cross-section of the DMFC anode with inlet and outlet manifolds. Based upon basic fluid dynamics for laminar flows, the resulting anode inlet velocity of the methanol aqueous solution can be calculated from a force balance between the retarding friction forces of flow through the channel and the net buoyancy force resulting from two-phase flow in the anode. This neglects the additional flow resulting from capillary forces acting on the mixture. The net force balance neglecting capillary forces can be shown as:

$$\rho_l g L = \rho_l g L(1-\alpha) + \frac{32}{D_a^2}\mu_l U_{in,a} L \qquad (2)$$

The last term on the right hand side describes the laminar flow resistance through the anode channel, and L is the channel length. In comparison, the flow resistance through the returning channel in the methanol circulation loop is negligible. The parameter α is the average void fraction within the anode channel, and is thus related to the cell current density, I, by:

$$\alpha = \frac{1}{U_{in,a} A_{ch}} \left(\frac{1}{2} \frac{RT}{P_{atm} - P_{sat}^{H_2O}} \frac{IA_{rxn}}{6F} \right) \quad (3)$$

In Eq. (3), the bracket denotes the average gas phase volumetric flow rate, which is proportional to the total electrochemical reaction rate (i.e. IA/6F on a molar basis). A_{rxn} represents the reaction area per channel, and is the current collecting rib width, plus the channel width, multiplied by the channel length. A simple homogeneous model has been assumed for the estimation of the void fraction. Solving Eqs.(2) and (3) simultaneously, one can readily determine the estimated methanol inlet velocity induced by the buoyancy forces. If capillary forces are present to aid the buoyancy forces, then a capillary pressure gradient, proportional to the void fraction gradient along the anode channel, should be added to Eq. (2). The resulting methanol inlet velocity will reflect the capillary-driven mechanism as well and be even higher providing additional methanol for DMFC operation.

The methanol flow rate given by Eq. (2) can be shown to correspond to a stoichiometric current density given by:

$$I_{stoich,a} = 6F \frac{A_{ch} U_{in,a} c_{in,a}^{MeOH}}{A_{rxn}} \quad (4)$$

From a comparison of the estimated stoichiometric current density with the design current density, one can then determine the anodic inlet stoichiometry at the design current density. The calculated anode flow rate also permits determination of the temperature rise in the anode solution from inlet to exit. Assuming that all waste heat generated from the cell is carried away by the liquid fuel, the fuel flow temperature rise can be shown as:

$$\Delta T_f = \frac{1}{\rho_l c_{p,l} U_{in,a} A_{ch}} \left(\frac{1}{\eta} - 1 \right) V_{cell} I A_{rxn} \quad (5)$$

where η is the energy efficiency of DMFC and can be assumed to be very close to ~0.3. For a cell electrical power output of 1 W, and an expected electrochemical efficiency of ~0.3, 2.33 W of energy will be dissipated as heat within the system. Assuming a natural convection coefficient of 25 W/m^{2}K, and an ambient temperature of 20^{o}C, up to 1.5 W would be dissipated from all six faces. This shows that proper insulation may not even be needed to maintain the fuel cell at a desired operating temperature, and that effective thermal control of the fuel cell within the desired operating range can be achieved with little or no effort. The remaining energy generated as a result of inefficiency in the electrochemical reaction must be dissipated from the cell. Considering the methanol also as a coolant, calculation of the expected temperature rise in the gravity-induced flow rate of methanol leads to a temperature rise of less than 2^{o}C for the highest power density condition, indicating that the cell can be effectively cooled by the liquid fuel itself. This confirms the belief that a DMFC of this size needs no external cooling as in a hydrogen PEM. Stable temperature operation would be ensured in a static environment with fuel cell insulation/radiation fins tailored to match the ambient conditions and desired operating temperature.

Figures 7 and 8 display results from the above calculations as a function of the cell current density at a cell operating temperature of 80 ^{o}C. It is shown in Figure 8 that the gravity-fed velocity can support an anode stoichiometric flow ratio as high as 70 for methanol concentrations as dilute as 0.2M, even without inclusion of capillary forces in the analysis. Based upon previous work with DMFC cells, this magnitude of the stoichiometric flow ratio will provide sufficiently large flow rates for DMFC operating at 100 mA/cm^2 (Mench et al. 2001).

Cathode Air Circulation via Thermal and Solutal Buoyancy Forces

Based upon natural convection and the fact that moist air will be lighter exiting the cathode that the dry air entering, the air cathode induced velocity can be shown as:

$$U_{in,c} = \frac{H^2}{12 \rho_{g,\infty} \nu_g} g \left\{ \rho_{g,\infty} - \left[1 - \beta (T - T_\infty) \right] \overline{\rho}_{g,c} \right\} \quad (6)$$

where H is the channel height and is $\overline{\rho}_{g,c}$ the average air density due to the moisture content which can be calculated as:

$$\overline{\rho}_{g,c} = \frac{1}{L} \left[\overline{\rho}_{g,0\_y_{sat}} y_{sat} + \rho_{g,sat} (L - y_{sat}) \right] \quad (7)$$

$$\frac{y_{sat}}{L} = \frac{A_{ch} U_{in,c} \left(\frac{P_{sat}^{H_2O}}{RT} - c_{g,\infty}^{H_2O} \right)}{\frac{IA_{rxn}}{F} \left[(0.5 + \alpha) - \frac{P_{sat}^{H_2O}}{P_{atm}} (0.25 + \alpha) \right]} \quad (8)$$

$$\rho_{g,sat} \approx \frac{P_{sat}^{H_2O}}{RT} M^{H_2O} + \frac{P_{atm} - P_{sat}^{H_2O}}{RT} M^{air} \quad (9)$$

In Eq. (8), y_{sat} is the distance along the channel flow path until the air is saturated with water vapor, and α represents the effective water transport coefficient per proton through the electrolyte membrane. Based upon literature, (e.g. Ren and Gottesfeld, 2001), α is estimated to be 2.5. Correspondingly, the cathode air-breathing stoichiometric current density is given by:

$$I_{stoich,c} = 0.21 \frac{P_{atm}}{RT_{\infty}} \frac{U_{in,c} A_{ch}}{A_{mn}} 4F \qquad (10)$$

Similar calculations can be made to determine ranges of flow velocities and stoichiometries supported by the cell design. Figures 9 and 10 show the calculated air velocity induced by thermal and solutal buoyancy forces in the DMFC cathode, and the corresponding stoichiometric current density at a cell operating temperature of 80°C. It is clear that it is possible to have a stoichiometric ratio between 2 and 3, depending on the choice of the channel length. This stoichiometry is sufficient to sustain the air cathode air operation. In order to facilitate a higher cathode stoichiometry, a cathode channel length of 0.3 or 0.5 cm can be realized by using an interrupted cathode channel design, namely breaking the entire cathode channel into 2 or 3 sections. This would alter Fig. 4 by breaking up the parallel flow channels into two or more sets of shorter parallel sections with inlets and exits to the sides of the fuel cell shown in Fig. 1. The resultant design would have a higher cathode stoichiometric ratio, but would not be significantly more complex.

CONCLUSIONS

The design of a micro direct methanol fuel cell system consisting of twenty cells with a total volume of 1 cm^3 and total projected power of 0.5 – 1 W was presented. The pump-less DMFC design is self-activated and terminating, and relies purely on natural thermal and solutal buoyancy forces. Calculations show that adequate anode and cathode stoichiometries can be achieved. This design is expected to be able to provide a several-fold increase in specific energy than the best lithium-based thin film battery.

REFERENCES

J. Bostaph, R. Koripella, A. Fisher, D. Zindel, J. Hallmark, and J. Neutzler, "Microfluidic fuel delivery for 100mW DMFC." *in Proc. of the symposium on direct methanol fuel cells*, the 199th Electrochemical Society Proceedings Series, Princeton, NJ, 2001.

G. Halpert, S. R. Narayanan, T. I. Valdez, W. Chun, H. Frank, A. Kinder, and S. Surampudi, "Progress with the direct methanol liquid-feed fuel cell system." *in Proc. of 32nd IECEC-97*, Vol. 2, pp.774-778, 1997.

S. C. Kelly, G. A. Deluga, and W. Smyrl, *Electrochemical and Solid State Letters*, Vol. 3, pp. 407-409, 2000.

M. M. Mench, S. Boslet, S. Thynell, J. Scott, and C. Y. Wang, "Experimental study of a direct methanol fuel cell." *in Proc. of the symposium on direct methanol fuel cells*, the 199th Electrochemical Society Proceedings Series, Princeton, NJ, 2001.

S. R Narayanan, F. Clara, and T. I. Valdez, "Development of a miniature direct methanol fuel cell system for cellular phone applications." *in Proc. of the symposium on direct methanol fuel cells*, the 199th Electrochemical Society Proceedings Series, Princeton, NJ, 2001.

X. Ren, and S. Gottesfeld, "Electro-osmotic Drag of Water in Poly(perfluorosulfonic acid) Membranes," *J. Electrochem. Soc.*, Vol. 148, pp. A87, 2000.

X. Ren, T. E. Springer, and S. Gottesfeld, "Water and methanol uptakes in Nafion membrane and membrane effects on direct methanol cell performance," *J. Electrochem. Soc.*, Vol. 147, pp. 96, 2000.

S. Surampudi, S. R. Narayanan, E. Vamos, H. Frank, G. Halpert, A. Laconti, J. Kosek, G. K. Surya, and G. A. Olah, *J. Power Sources*, Vol. 47, pp. 377, 1994.

C. Y. Wang, M. M. Mench, S. Thynell, Z. H. Wang and S. Boslet, "Computational and experimental study of direct methanol fuel cells." *Int. J. Transport Phenomena*, Vol. 3, August issue, 2001.

Table I. Dimensions of the DMFC Stack

Quantity	Value
Gas channel length	1 cm
Gas channel height	0.010 cm
Gas channel width	0.050 cm
Membrane electrode assembly thickness	0.020 cm
Current collector rib width	0.050 cm
Bipolar plate thickness	0.030 cm

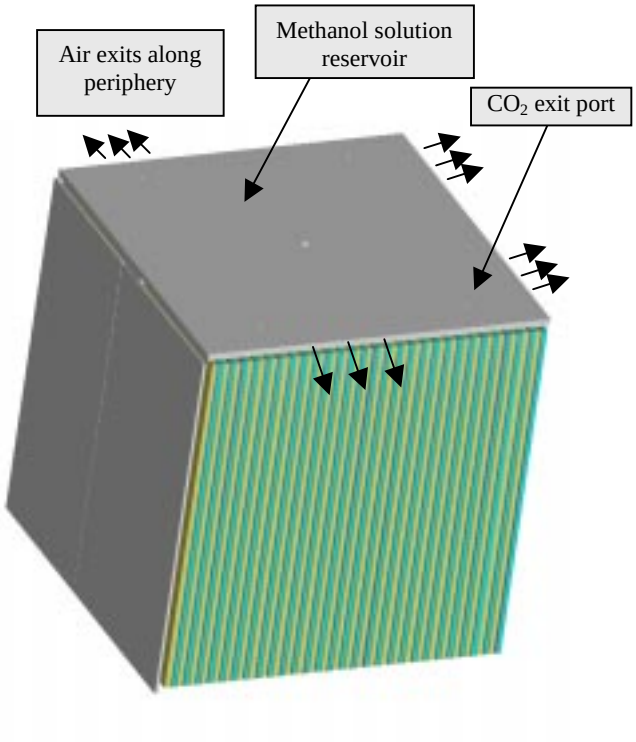

(a) Top Perspective

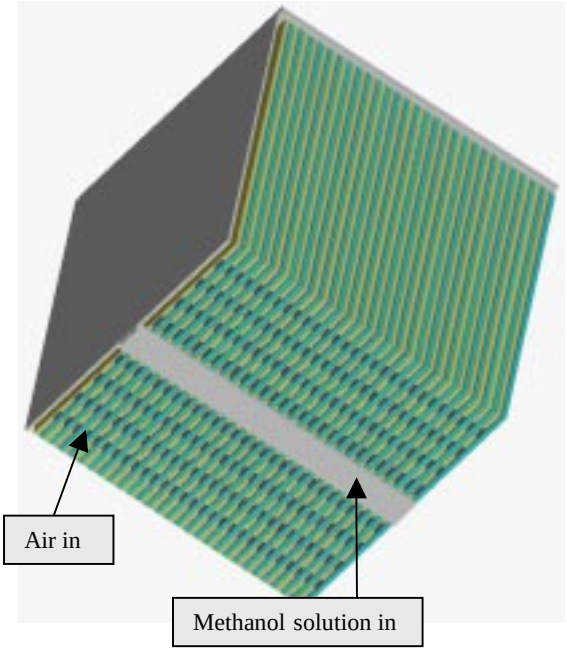

(b) Bottom Perspective

Figure 1. Schematic of proposed 1 cm^3 Direct Methanol Fuel Cell (DMFC) from different perspectives

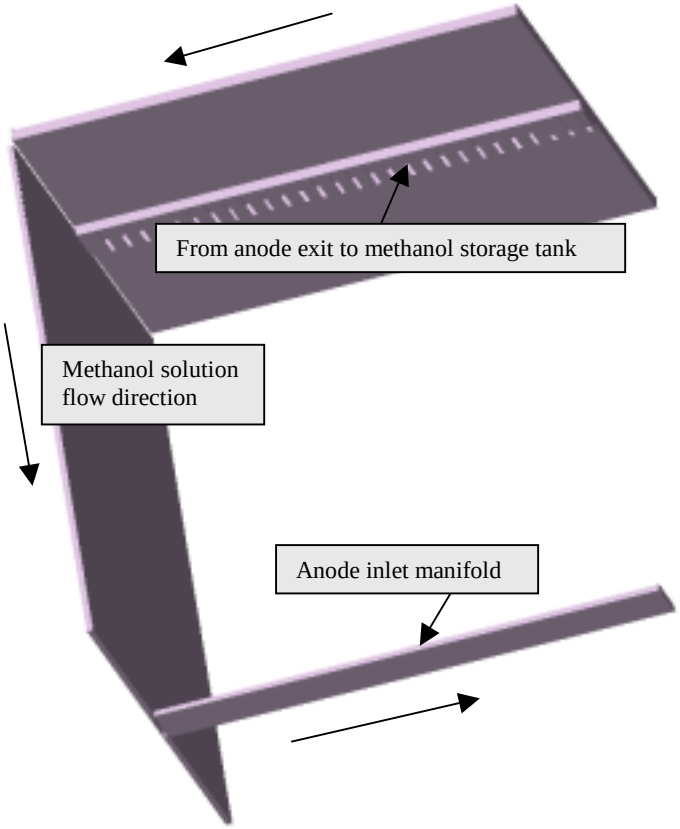

Figure 2. Schematic of methanol fuel supply tank, feed system, and interface with fuel cell

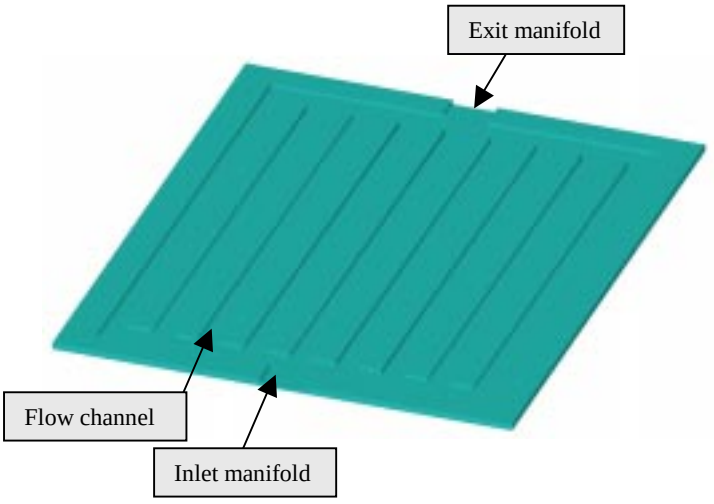

Figure 3. Schematic of anode flow plate

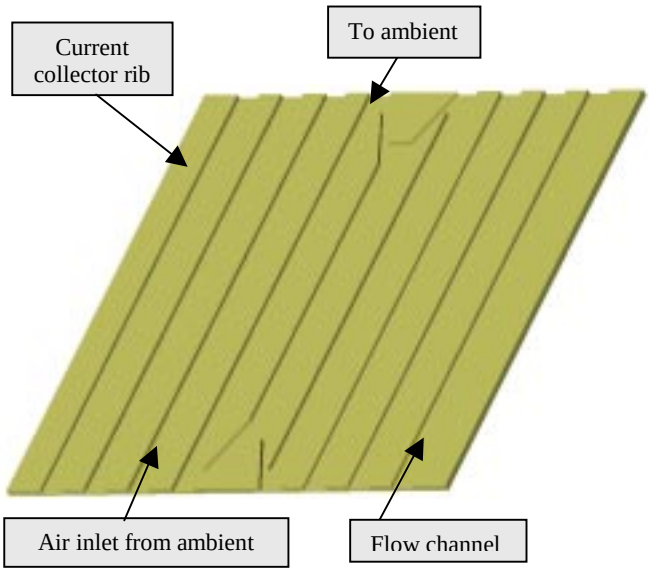

Figure 4. Schematic of cathode flow plate

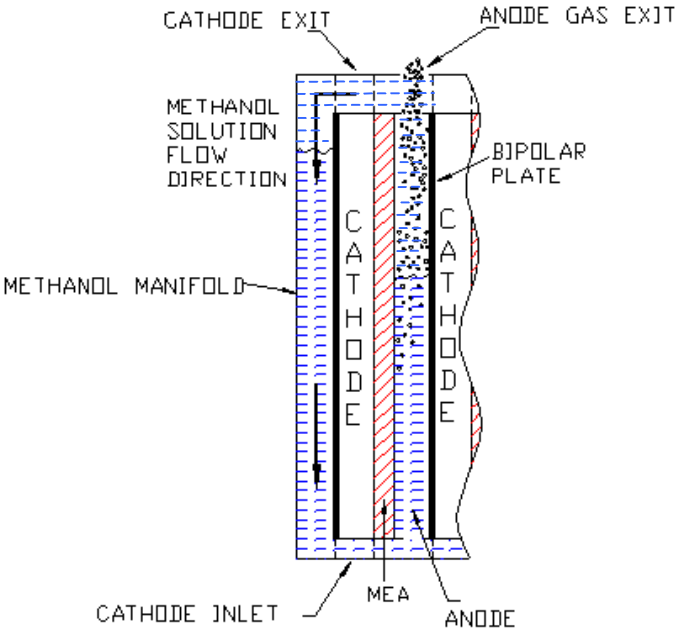

Figure 6. Cross-sectional view of 1 cm3 DMFC with inlet and outlet manifolds and fuel reservoir

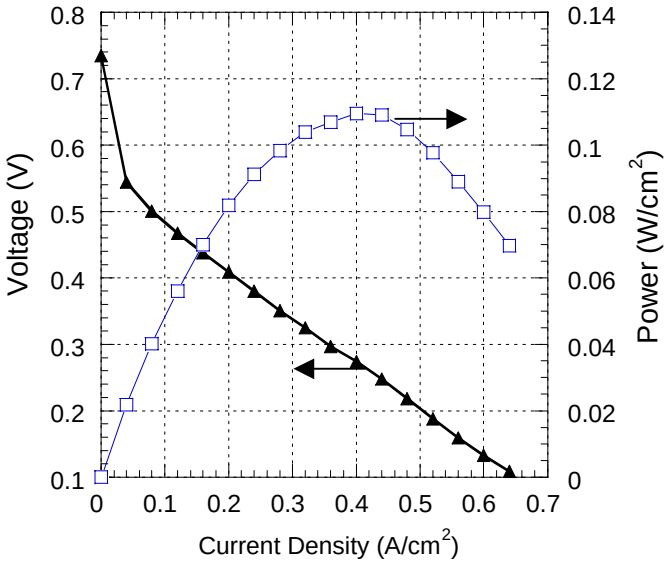

Figure 5. Polarization curve and power density for a 50 cm^2 DMFC under operating conditions: 1.0 M solution, anode flowrate: 20 mL/min, cathode air flowrate: 6000 mL/min, anode exit pressure: 1 atm, cathode exit pressure: 2.1 atm

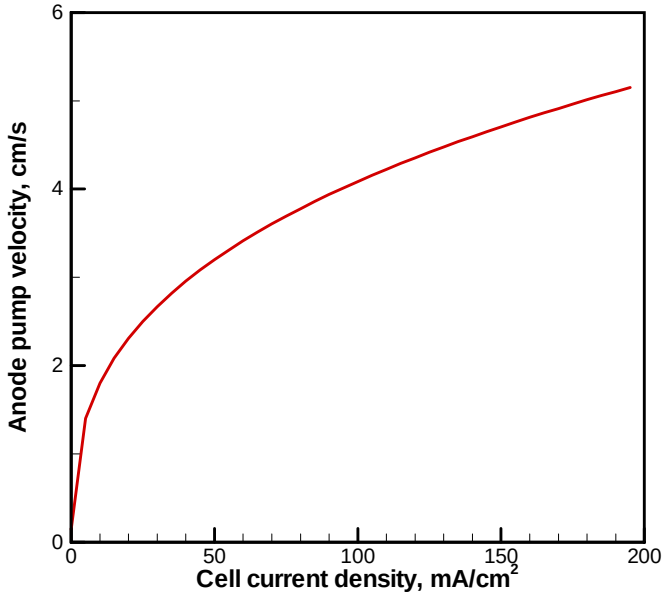

Figure 7. Calculated anode feed velocity based on buoyancy forces

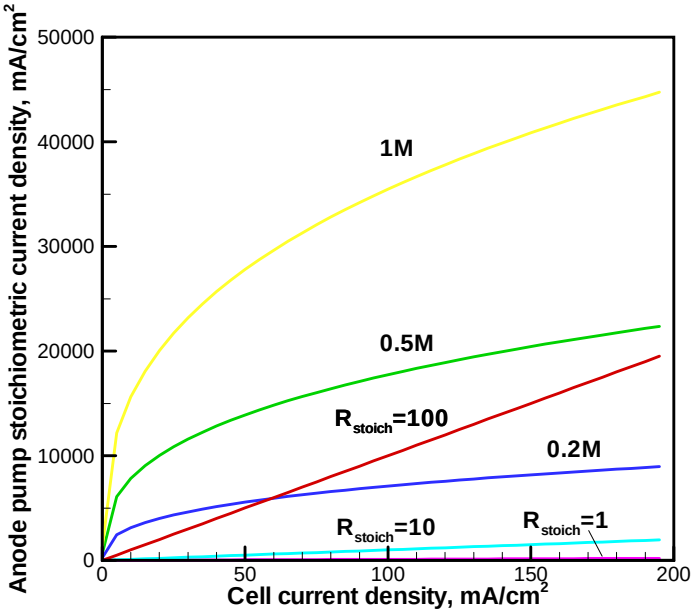

Figure 8. Anode feed stoichiometric current density, where the stoichiometric flow ratio of 1, 10 and 100 are also shown

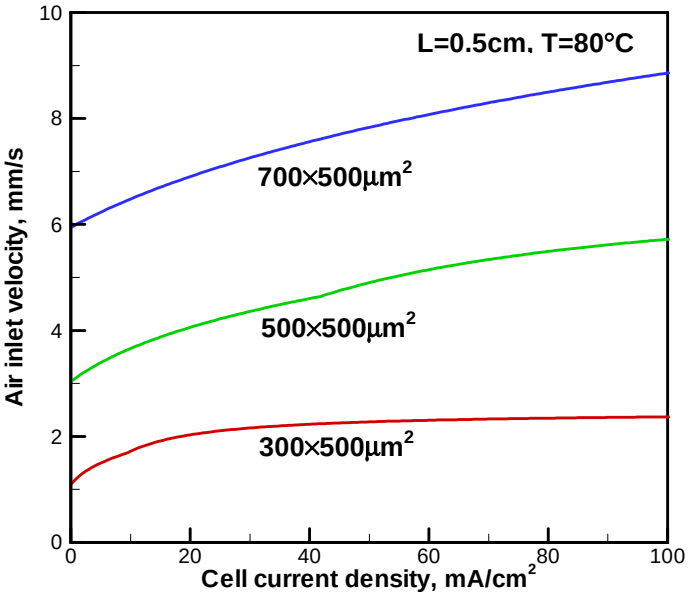

Figure 9. Calculated cathode air inlet velocity

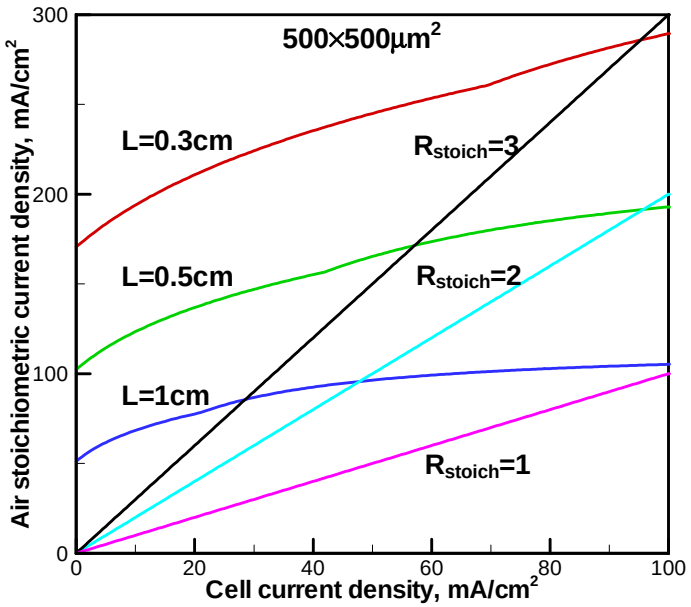

Figure 10. Air stoichiometry of cathode flow as a function of cell current density